

Study of the cyclen derivative 2-[1,4,7,10-tetraazacyclododecan-1-yl]-ethanethiol and its complexation behaviour towards d-transition metal ions

Sara Lacerda ^a, Maria Paula Campello ^a, Isabel C. Santos ^a,
Isabel Santos ^{a,*}, Rita Delgado ^{b,c}

^a Instituto Tecnológico e Nuclear, Estrada Nacional 10, 2686-953 Sacavém, Portugal

^b Instituto de Tecnologia Química e Biológica, UNL, Apartado 127, 2781-901 Oeiras, Portugal

^c Instituto Superior Técnico, Av. Rovisco Pais, 1049-001 Lisboa, Portugal

Received 12 March 2007; accepted 5 April 2007

Available online 8 May 2007

Abstract

The compound 2-[1,4,7,10-tetraazacyclododecan-1-yl]-ethanethiol (**L2**) has been synthesized and characterized by multinuclear NMR spectroscopy and mass spectrometry. Its thiol-protected precursor **L1** has also been isolated and characterized, including by X-ray structural analysis. The protonation constants of **L2** were determined by potentiometric methods at 25.0 °C and 0.10 mol dm⁻³ KNO₃ ionic strength. ¹³C NMR studies and 2D NMR spectra recorded at different pD values have been used to analyse its protonation scheme. Stability constants of **L2** with Cu²⁺, Zn²⁺ and Cd²⁺ were also determined by potentiometry, and the Zn(II) and Cu(II) complexes were studied in solution by NMR, UV–Vis, and EPR spectroscopies. The pM values (pH 7.4) calculated for the metal complexes of **L2** are higher than the corresponding values found for cyclen and cyclam, but the selectivity of **L2** for Cu²⁺ is low.

© 2007 Elsevier Ltd. All rights reserved.

Keywords: 2-Ethanethiol-cyclen derivative; Protonation constants; Stability constants; Protonation sequence; ¹³C NMR titration; EPR

1. Introduction

Copper offers an almost unique combination of radio-nuclides for imaging (^{60–62,64}Cu) and for targeted radio-nuclide therapy (^{64/67}Cu). The ⁶⁴Cu, due to its nuclear properties, is the most versatile of all copper radionuclides, being suitable both for positron emission tomography (PET) imaging (β^+ emission) and for targeted radiotherapy (β^- emission). Moreover, this duality offers the possibility of using PET to quantify *in vivo* the regional distribution of radioactivity, a crucial issue in the assessment of radiation dosimetry when planning targeted radionuclide therapy. Due to the well recognized preference of copper(II) for nitrogen and sulphur donor atoms, most of the studies

in the radiopharmaceutical field have involved open-chain nitrogen and/or sulphur chelators [1,2]. Concerning tetraazamacrocycles, the ones used for labelling peptides or antibodies with ^{64/67}Cu have mainly nitrogen and/or oxygen pendant arms [1,3]. To the best of our knowledge, the number of tetraazamacrocycles bearing thiol and/or thioether groups as pendant arms are scarce and some of them have been synthesized and coupled *in situ* to biologically active molecules, without being isolated and characterized [4,5].

As part of our ongoing research work on the synthesis and characterization of radiocomplexes with biological interest [6], we have synthesized and characterized a mono-*N*-substituted cyclen derivative with a 2-ethanethiol pendant arm, 2-[1,4,7,10-tetraazacyclododecan-1-yl]-ethanethiol (**L2**). This compound, although previously described as useful for site-specific labelling of proteins, has never been isolated in a pure form and/or characterized [4].

* Corresponding author. Tel.: +351 21 9946201; fax: +351 21 9946185.
E-mail address: isantos@itn.pt (I. Santos).

Herein, we report on the synthesis and characterization of **L2**, as well as on its thiol-protected precursor **L1**. Protonation constants of **L2** and its stability constants with Cu^{2+} , Zn^{2+} and Cd^{2+} will also be reported. An analysis of the protonation scheme of **L2** is discussed, as well as the structural environment in solution of Cu(II) and Zn(II) in the complexes with **L2**.

2. Experimental

2.1. Reagents

Chemicals and solvents were of reagent grade and were used without further purification, unless stated otherwise. 1,4,7,10-tetraazacyclododecane (cyclen) was purchased from Strem (New-Buryport, MA, USA). Sodium hydride, triphenylmethane-thiol, tetrahydrofuran, dibromoethane, toluene, sodium hydroxide, methanol, dichloromethane, ammonium, hydrochloride acid, deuterated water and chloroform were obtained from Aldrich Chemical Co. Silica gel 60 (70–230 mesh, pH range = 6.5–7.5) was obtained from Merck.

2.2. Analytical methods

^1H (300 MHz) and ^{13}C (75.5 MHz) NMR spectra were recorded in a Varian Unit Inova-300 spectrometer at a probe temperature of about 20°C. The spectra were performed in CDCl_3 (δ/ppm : ^1H : 7.24; ^{13}C : 77.00) or D_2O versus an external reference of 1,4-dioxane (δ/ppm : ^1H : 3.75; ^{13}C : 69.20). Positive-ion mass spectra were obtained in a Finnigan FT/MS 2001-DT FTICR mass spectrometer by laser desorption ionization. pH measurements were performed in a ORION SA 720. UV–Vis spectra were done in a Cary 500. EPR spectroscopic measurements of the copper complex were recorded with a Bruker ESP 380 spectrometer equipped with continuous-flow cryostats for liquid nitrogen, operating at X-band.

2.3. Synthesis of 2-[1,4,7,10-tetraazacyclododecan-1-yl]-ethanethiol (**L1**)

To a solution of cyclen (285 mg, 1.5 mmol) in hot toluene (50 cm^3) was slowly added bromoethyl tritylthiol [7] (210 mg; 0.5 mmol) dissolved in toluene (50 cm^3). The reaction mixture was refluxed overnight and then a solution of NaOH (20%) added. The organic phase was separated and the solvent evaporated under vacuo. The solid obtained was purified by silica-gel chromatography using as eluent a mixture of $\text{CHCl}_3/\text{MeOH}/\text{aq. NH}_3$ (gradient 100:0:0 \rightarrow 0:100:0 \rightarrow 0:80:20, $R_f = 0.2$ in 80:20 MeOH/aq. NH_3 solution) **L1** (100 mg, 43%); δ_{H} /(300 MHz, CDCl_3): 7.37 (6 H, d, aromatic protons), 7.26–7.14 (9 H, m, aromatic protons), 2.89–2.84 (4 H, m), 2.52–2.48 (8 H, m), 2.36–2.32 (8 H, m); δ_{C} (75.5 MHz, CDCl_3): 144.9 (Ph), 129.6 (Ph), 127.8 (Ph), 126.5 (Ph), 66.8 (SCPh_3), 53.5 ($\text{CH}_2\text{CH}_2\text{SCPh}_3$), 50.80 (C_{ring}), 46.9 (C_{ring}), 46.1 (C_{ring}), 44.9 (C_{ring}), 29.4 ($\text{CH}_2\text{CH}_2\text{SCPh}_3$).

2.4. Synthesis of 2-[1,4,7,10-tetraazacyclododecan-1-yl]-ethanethiol (**L2**)

Compound **L1** was refluxed in 20% HCl, for 2 h. After cooling to room temperature, the resulting solution was washed with dichloromethane, the aqueous extracts separated and vacuum dried yielding a white solid **L2** (75 mg, 80%). δ_{H} (300 MHz, D_2O , pD 1.05): 2.54 (2 H, t, C(1)H); 2.70 (2 H, t, C(2)H); 2.84 (4 H, t, C(3)H); 2.97 (4 H, br m, C(6)H); 3.07 (8 H, br m, C(4)H + C(5)H); δ_{C} (75.5 MHz, $\text{D}_2\text{O}/1,4\text{-dioxane}$, pD 1.05): 56.8 (C2); 50.3 (C3); 45.6 (C4); 44.4 (C6); 43.9 (C5); 22.0 (C1); m/z (LDI): calc. for $[\text{C}_{10}\text{H}_{25}\text{N}_4\text{S}]^+$: 233.179, $[\text{C}_{10}\text{H}_{24}\text{N}_4\text{S}^{23}\text{Na}]^+$: 255.161, $[\text{C}_{10}\text{H}_{25}\text{N}_4\text{S}^{39}\text{K}]^+$: 271.135; found: $[\text{M}+\text{H}]^+$: 233.191, $[\text{M}+\text{Na}]^+$: 255.156, $[\text{M}+\text{K}]^+$: 271.118.

2.5. X-ray crystal analyses

Crystal data for **L1**: $\text{C}_{29}\text{H}_{52}\text{N}_4\text{O}_{10}\text{S}_2$, $M_r = 680.87$, triclinic, space group $P\bar{1}$, $a = 8.1242(1)$, $b = 8.8600(1)$, $c = 27.0151(4)$ Å, $\alpha = 81.8670(10)$, $\beta = 82.1130(10)$, $\gamma = 63.9020(10)^\circ$, $U = 1722.57(4)$ Å³, $Z = 2$, $D_c = 1.313\text{ g cm}^{-3}$, μ (Mo $\text{K}\alpha$) = 1.260 mm^{-1} . Suitable colourless prismatic crystals ($0.40 \times 0.32 \times 0.06\text{ mm}$) were mounted in air on a goniometer head. X-ray diffraction experiments were performed with a Bruker AXS APEX CCD detector diffractometer using graphite monochromated Mo $\text{K}\alpha$ radiation ($\lambda = 0.71073$ Å), at 150 K in the ϕ and ω scans mode. A semi empirical absorption correction was carried out using SADABS [8].

Data collection, cell refinement and data reduction were done with the SMART and SAINT programs [9]. The structures were solved by direct methods using SIR97 [10] and refined by fullmatrix least-squares methods using the program SHELXL97 [11] using the winGX software package [12]. Non-hydrogen atoms were refined with anisotropic thermal parameters. The H atoms of the CH and CH_2 were placed at calculated positions using a riding model, with distances C–H = 0.95 Å (aromatic) and C–H = 0.99 Å (CH_2) and with $U_{\text{iso}}(\text{H}) = 1.2U_{\text{eq}}(\text{C})$ of the parent atom. The H atoms in the water, NH_2 and NH were located in difference Fourier maps and its coordinates and isotropic thermal parameters were refined.

The residual electronic density ranging from 0.393 to -0.392 e \AA^{-3} was within expected values. The final refinement of 472 parameters converged to final R and R_w indices $R_1 = 0.0408$ and $wR_2 = 0.0972$ for 7020 reflections with $I > 2\sigma(I)$. Molecular graphics were prepared using ORTEP 3 [13].

2.6. Potentiometric studies

2.6.1. Reagents and solutions

Metal ion solutions were prepared at about $2.5 \times 10^{-3}\text{ mol dm}^{-3}$ from the nitrate salts of the metals and were titrated using standard methods [14]. Deionized

(Millipore/Milli-Q System) distilled water was used. Carbonate-free solutions of the KOH titrant were obtained, maintained and discarded when the percentage of carbonate was about 0.5% of the total amount of base [15].

2.6.2. Equipment and work conditions

The equipment was used as described before [16]. The temperature was kept at 25.0 ± 0.1 °C, atmospheric CO₂ was excluded from the cell during the titrations by passing purified nitrogen across the top of the experimental solution in the reaction cell. The ionic strength of the solutions was kept at 0.10 mol dm^{-3} with KNO₃.

2.6.3. Measurements

The $[\text{H}^+]$ of the solutions was determined by the measurement of the electromotive force (emf) of the cell, $E = E^\circ + Q \log[\text{H}^+] + E_j$. E° , Q , E_j and $K_w = ([\text{H}^+][\text{OH}^-])$ were obtained as described previously [17]. The value of K_w was found equal to $10^{-13.80} (\text{mol dm}^{-3})^2$. The potentiometric equilibrium measurements were made on 25.00 cm^3 of $\approx 2.00 \times 10^{-3} \text{ mol dm}^{-3}$ ligand solutions diluted to a final volume of 30.00 cm^3 , in the absence of metal ions and in the presence of each metal ion for which the $C_M:C_L$ ratio was 1:1. A minimum of two replicate measurements was taken.

The emf data were taken after additions of 0.050 cm^3 increments of standard KOH solution, and after stabilization in this direction, equilibrium was then approached from the other direction adding standard nitric acid.

For determination of the stability constants, out-of-cell titrations were performed in the pH region from which the direct and back titrations were not superimposed. In such regions, independent vials each one at different pH were prepared and left to equilibrate in a water bath at 25.0 °C and the corresponding pH values checked every week till stabilization of the pH, which occurred generally within 2–4 weeks.

2.6.4. Calculation of equilibrium constants

Overall protonation constants, β_i^{H} were calculated by fitting the potentiometric data obtained for the free ligand with HYPERQUAD program [18]. Stability constants of the various species formed in solution were obtained from the experimental data corresponding to the titration of solutions of the different metal ions, each of them with different metal to ligand ratios, also using the HYPERQUAD program. The initial computations were obtained in the form of overall stability constants, $\beta_{M_m H_n L_l}$ values, $\beta_{M_m H_n L_l} = [M_m H_n L_l] / ([M]_m \times [H]_n \times [L]_l)$. Differences, in log units, between the values $\beta_{M(HL)}$ (or $\beta_{MLH_{-1}}$) and β_{ML} provide the stepwise reaction constants. The species considered in a particular model were those that could be justified by the principles of co-ordination chemistry. The errors quoted are the standard deviations of the overall stability constants given directly by the program for the input data, which include all the experimental points of all titration curves. The hydrolysis constants of the metal ions were

taken from the literature and kept constant for the calculations [19].

2.7. NMR studies

2.7.1. ¹³C NMR titration

The electrode was calibrated with standard buffer solutions and the final pD was calculated according to the equation $\text{pD} = \text{pH}^* + (0.40 \pm 0.02)$ [20], where pH^* corresponds to the reading of the pH meter. The solutions ($\approx 2 \times 10^{-3} \text{ M}$) used for the NMR titration measurements were made up in D₂O and the pD value was adjusted by adding DCl or CO₂-free KOD. The solutions were allowed to stabilize and the pD values were measured directly in the NMR-tube with a combination microelectrode Mettler-Toledo U402-M3-S7/200.

2.7.2. EPR studies

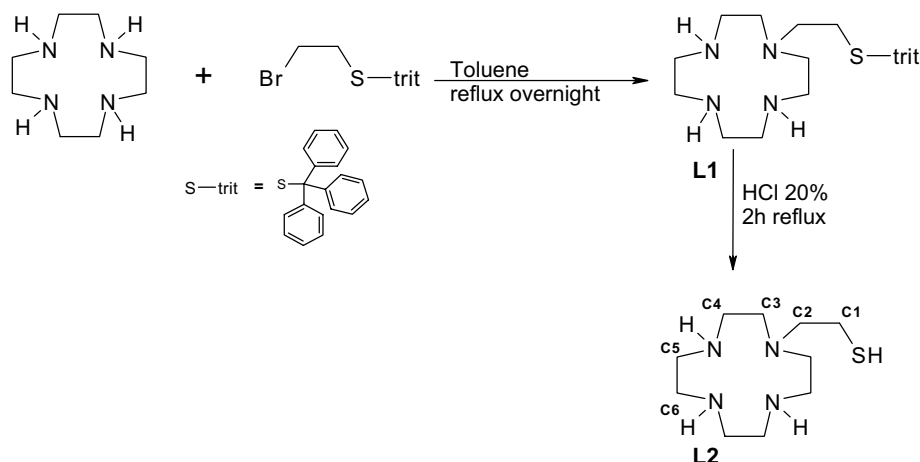
The Cu²⁺/L2 complexes ($\approx 1.6 \times 10^{-3} \text{ mol dm}^{-3}$ in 40% DMSO/H₂O solution) were prepared at pH 5, 8 and 12 and were recorded at 104 K. The EPR spectra of Cu²⁺/cyclen complexes were also recorded at the same pH values and conditions for comparison.

3. Results and discussion

3.1. Synthesis and characterization

Different synthetic procedures have been described to prepare mono-substituted tetraazamacrocycles, namely the introduction of the side chain on the amine before cyclization [21–23], pH controlled reactions [24], protection/deprotection methods [25] or alkylation of the macrocycle using an excess of the ligand versus the desired alkylating agent [26]. It has also been reported that it was possible to introduce one oxygen or sulphur pendant arm in the cyclen backbone by reacting cyclen with stoichiometric amounts of trimethylene oxide or ethylene sulphide, respectively [27,4,5a,5b,5c]. Following our previous work on tetraazamacrocycles, we have tried the synthesis of the mono-*N*-(2-ethanethiol) cyclen derivative (L2) following the described methodology [4]. In our hands, such synthetic procedure has never worked properly and compound L2 could never be isolated. L2 was synthesized in 40% overall yield, by slow addition of bromoethyl tritylthiol [7] to cyclen, in a 1:3 molar ratio, followed by acidic deprotection of the thiol group (Scheme 1).

Compound L1 was also isolated and characterized by ¹H and ¹³C NMR spectroscopy and by X-ray crystallography, upon purification by column chromatography using MeOH/NH₃ as eluent. Slow concentration of the fractions containing L1 led to crystals suitable for X-ray crystallography. Compound L1 crystallizes on the triclinic system, *P*1 space group, with cell parameters $a = 8.1242(1) \text{ \AA}$, $b = 8.8600(1) \text{ \AA}$, $c = 27.0151(4) \text{ \AA}$, $\alpha = 81.867(1)^\circ$, $\beta = 82.113(1)^\circ$, $\gamma = 63.902(1)^\circ$ and $V = 1722.57(4) \text{ \AA}^3$. The asymmetric unit contains one molecule of diprotonated

Scheme 1. Syntheses of **L1** and **L2**.

L1 ($C_{29}H_{40}N_4S$), one sulphate dianion (SO_4)²⁻ and six water molecules, given the molecular formula $[C_{29}H_{40}N_4S] \cdot SO_4 \cdot 6H_2O$. In Fig. 1 is presented an ORTEP diagram showing the numbering scheme of the asymmetric unit.

Some selected bond lengths (Å) and angles (°) for the dication $[C_{29}H_{40}N_4S]^{2+}$ are listed in Table 1.

The macrocycle was found to be protonated in the amines N2 and N4. The average C–N_{protonated} bond distances (1.490 Å) are slightly longer than the average C–N_{unprotonated} ones (1.467 Å). These differences compare well with the values previously reported for other protonated macrocyclic ligands [28]. The four nitrogen atoms of the macrocycle are coplanar with an rms of 0.0306, the CH₂ groups of the backbone are below this plane, while the sulphur arm is above the plane, pointing in the opposite direction. The calculated torsion angle N1–C2–C1–S1 of 178.1° shows the relative position of the pendant arm towards the macrocycle cavity.

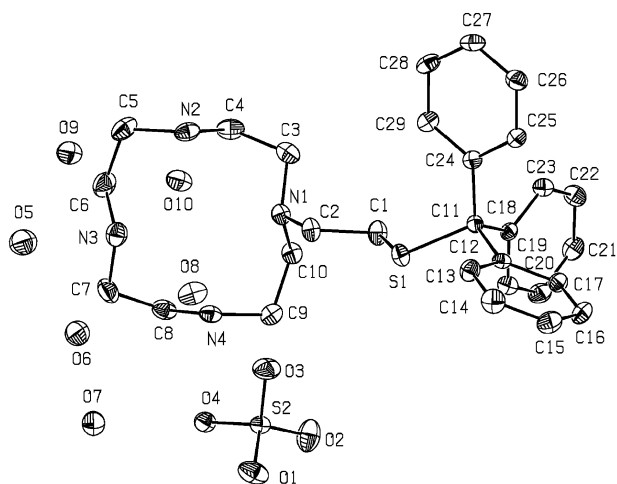


Fig. 1. ORTEP diagram with atomic numbering scheme of asymmetric unit with thermal ellipsoids at 50% probability level. Hydrogen atoms are omitted for clarity.

Table 1
Selected bond lengths (Å) and angles (°) for the dication $[C_{29}H_{40}N_4S]^{2+}$

S(1)–C(1)	1.822(2)	N(2)–C(4)	1.484(3)
S(1)–C(11)	1.862(2)	N(2)–C(5)	1.497(3)
C(1)–C(2)	1.531(2)	N(3)–C(6)	1.459(3)
N(1)–C(2)	1.470(2)	N(3)–C(7)	1.471(3)
N(1)–C(3)	1.472(2)	N(4)–C(8)	1.483(2)
N(1)–C(10)	1.467(2)	N(4)–C(9)	1.497(2)
C(1)–S(1)–C(11)	105.14(8)	C(2)–C(1)–S(1)	105.56(12)
C(10)–N(1)–C(3)	111.02(14)	N(1)–C(2)–C(1)	116.56(15)
C(5)–N(2)–C(4)	117.13(16)	C(3)–N(1)–C(2)	113.99(15)
C(7)–N(3)–C(6)	113.57(16)	C(10)–N(1)–C(2)	115.64(14)
C(8)–N(4)–C(9)	114.98(15)		

The crystal packing of compound **L1** is characterized (Fig. 2) by the formation of a bidimensional layer parallel to the bc plane due to several hydrogen bonds between the water molecules and due to intermolecular short N \cdots O and C \cdots O contacts between SO_4^{2-} units and the macrocycle (Table 2).

Compound **L2** is quite soluble in water and stable under aerobic conditions. The formulation of **L2** was mainly based on multinuclear NMR spectroscopy (¹H, ¹³C, ¹H,¹H COSY, ¹H,¹³C HSQC) at different pD values (range 1–14) and also on mass spectrometry. In the LDI-positive mass spectrum three main peaks were found at *m/z* = 233.191, 255.156 and 271.118 corresponding to $[M+H]^+$, $[M+Na]^+$ and $[M+K]^+$, respectively.

In the pD range studied, the ¹³C NMR spectra recorded exhibit six resonances, a pattern consistent with the two-fold symmetry expected for **L2**: four resonances were assigned to the carbon atoms of the backbone and the other two to the carbon atoms of the pendant arm. The ¹H NMR spectra at pD 1.05 presented five resonances with different multiplicities at 2.54, 2.70, 2.84, 2.97, 3.07 ppm in an intensity ratio of 2:2:4:4:8. At higher pD values, the ¹H NMR spectra became less clear due to the overlapping of some resonances. 2D NMR studies (¹H,¹H and ¹H,¹³C correlations) were performed at pD 1.05. In Fig. 3 is shown

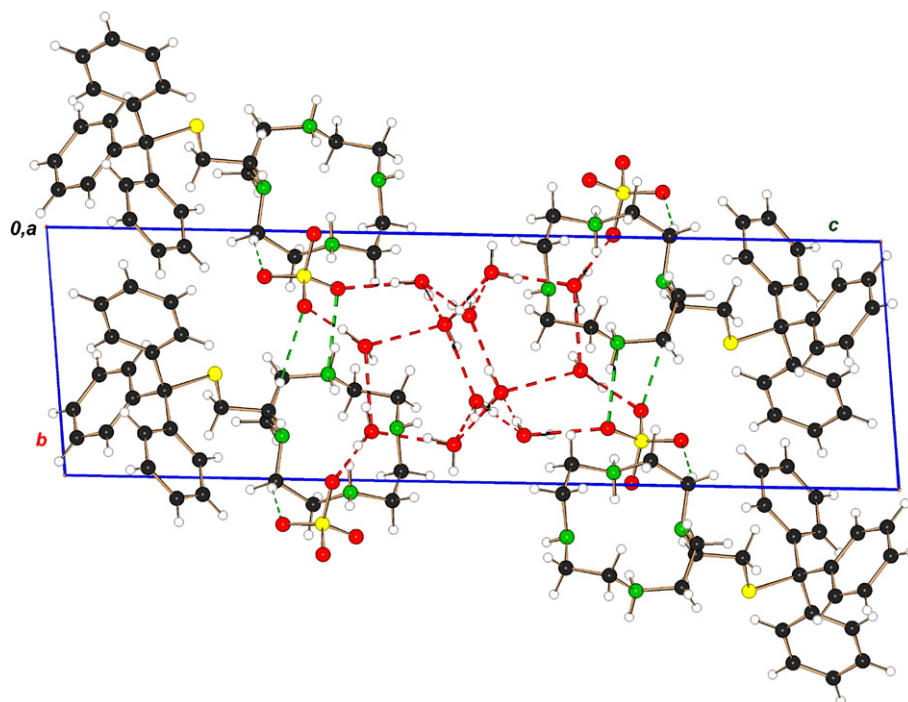
Fig. 2. Crystal structure of **L1** viewed along *a*.

Table 2
Selected hydrogen bonds and short contacts in the crystal structure of compound **L1**

	Distance (Å)
$O_{\text{sulphate}} \cdots N$	
O4...N4	2.766(2)
O4...N2	2.764(3)
$O_{\text{sulphate}} \cdots H\text{-}C_{\text{backbone}}$	
O1...H4b-C4	2.612(2)
O1...H6b-C6	2.381(2)
O3...H2a-C2	2.564(1)
$O_{\text{sulphate}} \cdots H\text{-}C_{\text{aromatic}}$	
O2...H14-C14	2.456(2)
O2...H28-C28	2.688(2)

the *g*-COSY ^1H , ^1H and the *g*-HSQC ^1H , ^{13}C 2D correlations. From these studies it was possible to conclude that the triplets centered at 2.54 and 2.70 ppm correlate with the carbons at 22.03 and 56.81 ppm, respectively. Based on the carbon and proton NMR data of the free arm and on literature data, the resonances at 22.03 and 56.81 ppm were assigned to the α (C1) and β (C2) carbon atoms of the pendant arm, respectively (Scheme 1). The triplet centred at 2.84 ppm (4 H) correlates with the carbon atoms at 50.26 ppm, assigned to C3. The multiplet at 2.97 ppm (4 H) correlates with the carbon atom at 44.39 ppm and correlates with the multiplet at 3.07 ppm (8 H). Based on these data the resonance at 44.39 ppm was assigned to the C6 carbon atoms and the multiplet at 3.07 ppm (8 H) was assigned to the protons bound to the C4 and C5 atoms which appear at 45.64 and 43.92 ppm,

respectively. In Table 3 are presented the chemical shifts and the corresponding assignment of the resonances of **L2** at pD 1.05.

3.2. Acid–base behaviour

The protonation constants of **L2** were determined by potentiometry at 25.0 °C and 0.10 mol dm $^{-3}$ KNO $_3$ ionic strength. The values found are summarized in Table 4. Compound **L2** has five protonation constants, from which four could be determined by potentiometry, but the remaining one is too low to be determined by this technique. Just for comparison, in Table 4 are also shown the protonation constants for cyclen, 2-hydroxyethyl cyclen (**L3**) and 3-hydroxypropyl cyclen (**L4**) (Fig. 4) [27,29].

Based on the values of Table 4 it is difficult to ascribe the protonation sequence of **L2**. In order to understand this sequence a ^{13}C NMR titration was performed. These studies were carried out at 20 °C without controlling the ionic strength [30]. In Fig. 5 are shown the ^{13}C NMR titration curves.

The ^{13}C NMR spectra recorded for **L2** exhibit six resonances in the entire pD range. For each magnetically equivalent carbon atom, single resonances have been observed, indicating a rapid exchange between protonated species. For the interpretation of these data, the pK_{H} values determined for **L2** (Table 4) were converted in terms of pK_{D} , using the correlation $pK_{\text{D}} = 0.11 + 1.10pK_{\text{H}}$, determined for polyaza and polyoxa–polyaza macrocyclic compounds by Delgado et al. [31]: $pK_{\text{D}1} = 12.19$, $pK_{\text{D}2} = 11.09$, $pK_{\text{D}3} = 9.08$ and $pK_{\text{D}4} = 2.62$. From the analysis of the

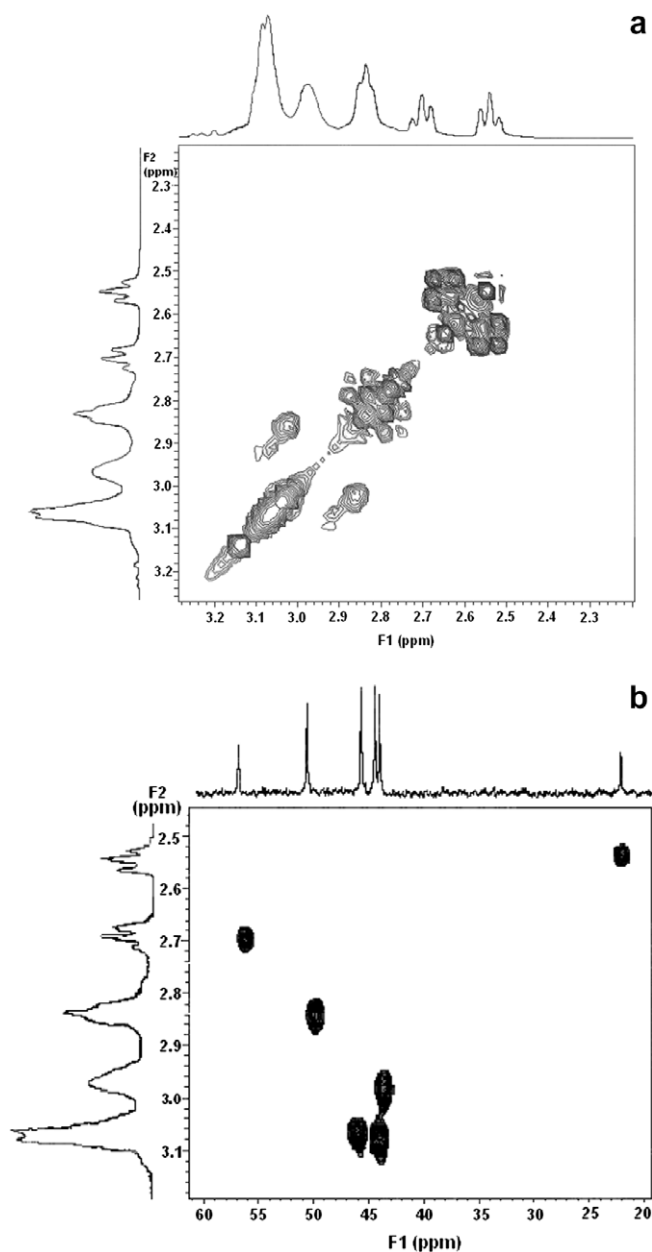


Fig. 3. g-Cosy ^1H , ^1H (a) and g-HSQC ^1H , ^{13}C (b) 2D correlations for **L2** at pD 1.05.

Table 3
 ^1H and ^{13}C NMR data for **L2** at pD 1.05

Assignment	Chemical shift (ppm)	
	^1H	^{13}C
C1	2.54 (t, 2 H)	22.03
C2	2.70 (t, 2 H)	56.81
C3	2.84 (t, 4 H)	50.26
C4	3.07 (m, 8 H)	45.64
C5		43.92
C6	2.97 (m, 4 H)	44.39

NMR titration curves, three pD regions were defined, one comprising two protonation constants ($13.0 \geq \text{pD} \geq 10.5$), and the other two comprising one protonation constant each ($10.5 \geq \text{pD} \geq 8.0$ and $\text{pD} \leq 3.0$). The high

Table 4
Protonation constants (log units) of **L2** and other related macrocyclic ligands

Species <i>h, l</i>	L2 ^a		Cyclen ^b	L3 ^c	L4 ^d
	$\log \beta_{\text{H,L}}$	$\log K_{\text{H,L}}$	$\log K_{\text{H,L}}$	$\log K_{\text{H,L}}$	$\log K_{\text{H,L}}$
11	10.98(2)	10.98	10.97	10.72	10.56(4)
12	20.96(2)	9.98	9.87	9.28	9.14(4)
13	29.11(4)	8.15	1.6	<2	<2.3
14	31.39(6)	2.28	0.8	<2	<2.3
Overall basicity		31.39	23.24	<24	<24.4

Values in parentheses are standard deviations in the last significant figures.
^a $T = 25.0\text{ }^\circ\text{C}$, $I = 0.10\text{ mol dm}^{-3}$ in KNO_3 , this work.

^b $I = 0.50\text{ mol dm}^{-3}$ in KNO_3 , Ref. [29a] and $I = 0.20\text{ mol dm}^{-3}$ in NaClO_4 , Ref. [29b].

^c $I = 0.10\text{ mol dm}^{-3}$ NEt_4ClO_4 , Ref. [29c].

^d $I = 0.10\text{ mol dm}^{-3}$ in NaClO_4 , Ref. [27].

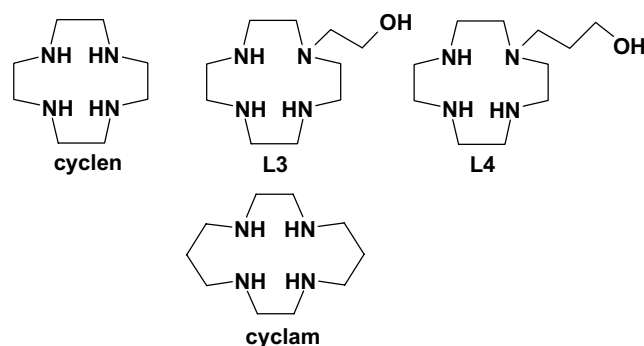


Fig. 4. Structure of the ligands used for comparison: cyclen, 2-hydroxyethyl cyclen (**L3**), 3-hydroxypropyl cyclen (**L4**) and cyclam.

symmetry of **L2** makes difficult to predict the protonation sequence, but an attempt has been made taking into account that when a protonation occurs at a given site the β -carbons are upfield shifted [32]. In the $13.0 \geq \text{pD} \geq 10.5$ region two protonations occur, and their constant values differ only by one log unit, which makes difficult to distinguish the effect of each one. However, taking into account that in this range the resonances **C2**, **C4** and **C5** are upfield shifted, while **C1** shifts downfield, it seems that the thiolate group is protonated and a second proton may be shared by the N_I and N_{III} amines. In the region $10.5 \geq \text{pD} \geq 8.0$ a third protonation occurs on one amine of the macrocyclic ring, and this proton together with the one already existing in the macrocycle backbone will be shared by the $\text{N}_I/\text{N}_{II}/\text{N}_{III}$ amines centres. This is supported by the upfield shift of the resonances **C1**, **C3**, and **C6**. In the pD range $8.0\text{--}3.0$ no significant changes were observed, but for $\text{pD} \leq 3.0$ the **C1**, **C4** and **C5** carbon atoms are upfield shifted, being **C1** the most significantly shifted (ca. 1 ppm), which may indicate the protonation of the N_I centre.

3.3. Stability constants

The complexation of **L2** with Cu^{2+} , Zn^{2+} and Cd^{2+} was followed by potentiometry, at $25.0\text{ }^\circ\text{C}$ and 0.1 mol dm^{-3}

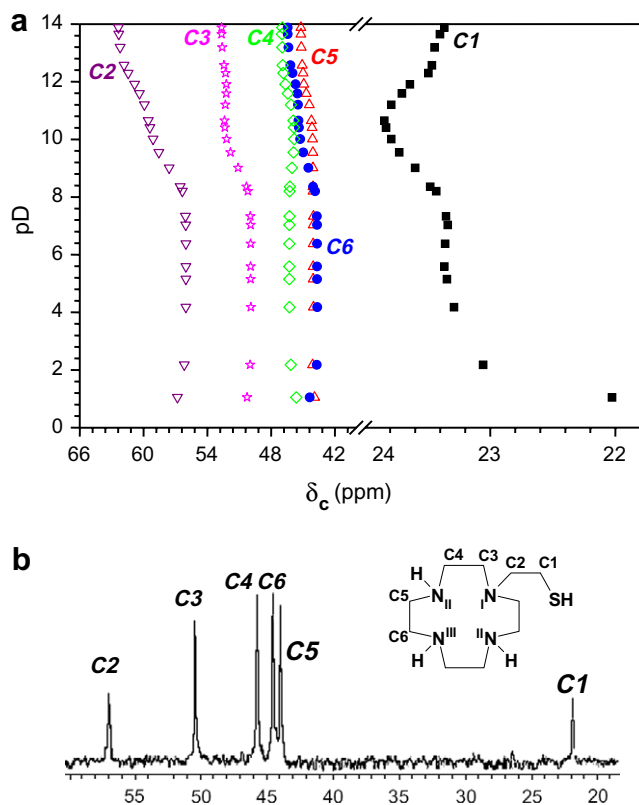


Fig. 5. (a) ^{13}C NMR titration curves for **L2** (chemical shift (δ_{C}) in function of pD): ■, C1; ▽, C2; ☆, C3; ◆, C4; △, C5 and ●, C6. (b) ^{13}C NMR spectrum of **L2** (D_2O , pD 1.05).

KNO_3 , and the corresponding stability constants were determined. The kinetics of formation of the complexes of **L2** with the transition metal ions studied is relatively slow. The stability constants were determined by the use

of a batch method in the pH regions where complexation equilibrium was not attained during in-cell titrations, leading to stability constants with relatively high standard deviations. In Table 5 are listed the stability constants of the complexes of **L2** with Cu^{2+} , Zn^{2+} and Cd^{2+} , together with the constants for the corresponding complexes with related tetraazamacrocycles. Cyclam was included due to its very high affinity for copper(II) [33].

Only mononuclear species were formed with the studied metal ions, namely $[\text{ML}]$, $[\text{M}(\text{HL})]$, $[\text{M}(\text{H}_2\text{L})]$, $[\text{M}(\text{L}(\text{OH}))]$ and $[\text{M}(\text{L}(\text{OH})_2)]$. The latter species is only formed for Cd^{2+} , while $[\text{M}(\text{H}_2\text{L})]$ only exists when $\text{M} = \text{Cu}^{2+}$. At physiological pH, the $[\text{ML}]$ complex is formed at about 100% for Cu^{2+} , while for Cd^{2+} and for Zn^{2+} only above pH 8 this is the main species (Fig. 6).

The trend found for the stability of the complexes studied, $[\text{CuL}] > [\text{ZnL}] \approx [\text{CdL}]$, follows the usual order for cyclen derivatives. However the $\log K_{\text{CuL}}/\log K_{\text{ZnL}}$ and $\log K_{\text{CuL}}/\log K_{\text{CdL}}$ ratios are smaller than usually found for ligands having only amine donor atoms, such as cyclen and cyclam. This feature, together with the larger values of K_{ML} observed for **L2**, when compared to cyclen, strongly suggests the involvement of the arm in the coordination sphere of the metal centre. For all the metal ions, completely different direct and backtitration potentiometric curves were obtained, suggesting structural rearrangements, may be related with the formation and break of the M–S bond.

A direct comparison of stability constants of **L2** and those reported for cyclen, **L3**, **L4** and cyclam can only be made using the pM ($-\log[\text{M}^{2+}]$) values (Table 6) [35], due to the different basicity of the ligands.

These data indicate that compound **L2** has higher affinity for the transition metal ions studied than the tetraaza-

Table 5

Stability constants (log units) for complexes of **L2** and other related ligands with Cu^{2+} , Zn^{2+} and Cd^{2+} ions

Metal	Species <i>mhl</i>	L2 ^a		Cyclen ^b	L4 ^c	Cyclam ^d
		$\log \beta_{\text{MHL}}$	$\log K_{\text{MHL}}$	$\log K_{\text{MHL}}$	$\log K_{\text{MHL}}$	$\log K_{\text{MHL}}$
Cu^{2+}	101	21.19(6)	21.17	23.29 24.8	17.3(1)	26.5 27.2
	111	27.45(4)	6.26			
	121	30.47(7)	3.02			
	1–11	12.2(1)	–8.99		10.2	
Zn^{2+}	101	18.6(1)	18.6	16.2 5.74	13.7(1)	15.5 3.99
	111	25.60(2)	7.00			
	1–11	8.8(1)	–9.8		–8.3	
Cd^{2+}	101	18.8(1)	18.8	14.3	13.0(1)	11.23
	111	25.51(5)	6.71			
	121				9.8	
	1–11	9.2(1)	–9.6			
	1–21	–1.7(1)	–10.9			

Values in parentheses are standard deviations in the last significant figures.

^a This work, $T = 25.0\text{ }^\circ\text{C}$, $I = 0.10\text{ mol dm}^{-3}\text{ KNO}_3$.

^b $I = 0.1\text{ mol dm}^{-3}\text{ NaNO}_3$, Ref. [29a].

^c $T = 25.0\text{ }^\circ\text{C}$, $I = 0.1\text{ mol dm}^{-3}\text{ NEt}_4\text{ClO}_4$, Ref. [27].

^d Refs. [33,34].

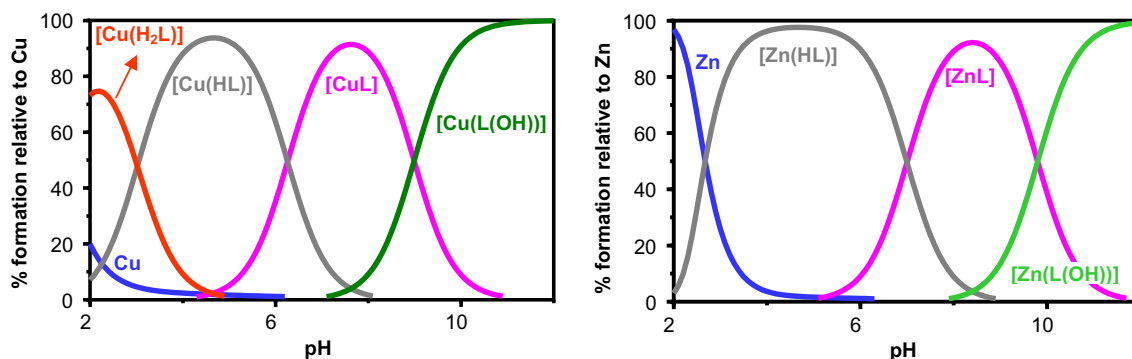


Fig. 6. Species distribution diagrams for the Cu^{2+} and Zn^{2+} complexes with **L2** in water, $C_L = C_M = 4.0 \times 10^{-5} \text{ mol dm}^{-3}$ (charges were omitted).

Table 6
pM values^a calculated for **L2** and other related ligands (pH 7.4)

Ion	L2	Cyclen	L4	Cyclam
Cu^{2+}	14.24	9.27, 10.02	11.59	10.19, 10.54
Cd^{2+}	11.91	4.73	7.29	2.57
Zn^{2+}	11.77	5.68	7.99	2.42

^a The values were calculated for 100% excess of free ligand, using the program HySS [35], $C_L = 2C_M = 1 \times 10^{-5} \text{ mol dm}^{-3}$ and the stability constants given in Table 5.

macrocycles considered for comparison. For the same cavity size, the presence of a coordinating pendant arm increases significantly the stability of the complexes. A decrease of the pM values is found when the cavity size increases. However, **L2** shows a low selectivity for Cu over Zn and Cd.

3.4. Structural studies in solution

3.4.1. NMR studies of zinc(II) complexes

To assess the nature of the inner sphere of the zinc, the ¹³C NMR spectra of solutions containing Zn^{2+} and **L2** (1:1 molar ratio) have been recorded at different pD values. Based on the species distribution diagram (Fig. 6), we have chosen the 5.6, 7.6 and 11.6 pH values, which correspond to the [Zn(HL)], [ZnL] and [Zn(L(OH))] species, respectively. In Table 7 are collected the chemical shifts of the carbon atoms of the $\text{Zn}^{2+}/\text{L2}$ species formed as well as those for the free **L2**, recorded in the same experimental conditions.

Table 7
Chemical shift (δ/ppm) of the carbon atoms of **L2** and of the species Zn/L2 at pD 6, 8 and 12

	pD \approx 6		pD \approx 8		pD \approx 12	
	L2	Zn/L2	L2	Zn/L2	L2	Zn/L2
C1	23.36	26.37	23.43	26.02	23.64	25.97
C2	56.02	55.07	56.36	57.22	60.84	57.18
C3	49.93	51.66	50.20	52.22	52.22	52.18
C4	46.30	46.54	46.26	47.22	46.66	47.19
C5	44.04	45.64	44.05	46.18	44.93	44.45
C6	43.69	44.40	43.87	44.49	45.71	46.14

Most of the carbon atoms of **L2** are significantly downfield shifted upon coordination to the Zn^{2+} . These results are consistent with the formation of a $\text{Zn}^{2+}/\text{L2}$ complex and seem to indicate that all the donor atoms are coordinated to the metal. The significant downfield shift observed for **C2**, when pD increases from 6 to 8, may be correlated to the deprotonation followed by coordination of the thiol group, in agreement with the potentiometric studies (Table 5).

3.4.2. UV–Vis and EPR spectroscopic studies of copper(II) complexes

The UV–Vis–NIR and the EPR spectra of $\text{Cu}^{2+}/\text{L2}$ and $\text{Cu}^{2+}/\text{cyclen}$ complexes were recorded at pH 5, 8 and 12, which for $\text{Cu}^{2+}/\text{L2}$ corresponds to about 100% of the [Cu(HL)], [CuL] and [Cu(L(OH))] species, respectively (Fig. 6). As can be seen in Table 8, the electronic spectra of the Cu^{2+} complexes with **L2** and cyclen exhibit two well defined bands, one in the UV–Vis range and another in the charge transfer region. A red-shift of the band in the UV–Vis is expected when the geometry of a Cu^{2+} complex changes from a square planar to a penta-coordinated one. For $\text{Cu}^{2+}/\text{cyclam}$ [36] and $\text{Cu}^{2+}/1,4,8\text{-trimethyl-11-(2-thioethyl)-1,4,8,11-tetraazacyclotetradecane}$ [5a], which have been considered to be four and five-coordinated, the maximum absorption of the bands has been reported to be at $\lambda_{\text{max}} = 513 \text{ nm}$ and 622 nm , respectively. Our data for $\text{Cu}^{2+}/\text{L2}$ and $\text{Cu}^{2+}/\text{cyclen}$ seem to indicate that in the complexes studied in this work the copper centre is five-coordinated. In the pH range studied, both complexes present the same pattern for the UV–Vis spectra and the maximum of absorption does not change significantly with the pH. These results may suggest that the environment around the Cu is the same, independently of the protonation of the corresponding ligand. However, the molar absorptivity of the complex $\text{Cu}^{2+}/\text{L2}$ increases with pH, indicating a highest distortion for the complex, most probably due to the deprotonation of the sulphur atom and formation of a strong apical Cu–S bond.

In Fig. 7 are shown the X-band EPR spectra of $\text{Cu}^{2+}/\text{L2}$ and $\text{Cu}^{2+}/\text{cyclen}$ complexes and their simulated spectra, at different pH values. All the spectra indicated the presence

Table 8
Spectroscopic data for the copper(II) complexes of **L2** and other related ligands taken from literature

Ligands or Cu(II) complexes (pH)	UV–Vis–near IR λ/nm ($\epsilon/\text{mol}^{-1} \text{dm}^3 \text{cm}^{-1}$)	EPR ($10^4 A_i/\text{cm}^{-1}$)					
		g_x	g_y	g_z	A_x	A_y	A_z
L2 (5) ^{a, b}	612 (112); 277 (4×10^4)			2.198			182.14
L2 (8) ^a	615 (132); 270 (6×10^4)	2.040	2.055	2.198	16.88	17.68	182.41
L2 (12) ^a	620 (220); 273 (8×10^4)	2.041	2.082	2.200	1.92	7.68	186.98
Cyclen (5) ^a	579 (56); 282 (1×10^4)	2.040	2.055	2.197	16.88	21.02	181.97
Cyclen (8) ^a	578 (56); 274 (3×10^4)	2.040	2.055	2.196	16.88	21.02	181.99
Cyclen (12) ^a	581 (80); 274 (3×10^4)	2.052	2.060	2.212	2.30	10.33	180.23
[Cu(cyclen)Cl] ⁺ ^c	599 (220)	2.057		2.198	24.1		184.2
[Cu(cyclam)]Cl ₂ ²⁺	513 (100)	2.049		2.186	38.7		205.0
[Cu(H ₂ O) ₆] ²⁺ ^d		2.08		2.4			134.0

^a This work.

^b Species A: $g_z = 2.410$ and $A_z = 131.92$.

^c Ref. [36].

^d Ref. [38].

of only one species, except for $\text{Cu}^{2+}/\mathbf{L2}$ at pH 5, which revealed the presence of two species. All the spectra showed the expected four well-resolved lines at low field, due to the interaction of the unpaired electron spin with the copper nucleus. The hyperfine coupling constants (A) and g values obtained by the simulation of the spectra [37] are shown in Table 8, together with those of other copper(II) complexes taken from literature, for comparison [36,38]. The simulation of the spectra revealed three different g values with

$g_z > (g_x + g_y)/2$ and the lowest $g \geq 2.04$, which is characteristic of mononuclear copper(II) complexes having rhombic-octahedral with elongation of the axial bonds or distorted square-based pyramidal symmetries, and $d_{x^2-y^2}$ ground state.

The two species present, at pH 5, in the EPR spectrum of $\text{Cu}^{2+}/\mathbf{L2}$ are in about the same proportion, based on the intensity of the bands. The simulation of this spectrum could not be obtained and so is not presented. Nevertheless, the direct analysis of the spectrum and the estimated g_z and A_z parameters suggest that one species (species A) corresponds to the aqua-complex $[\text{Cu}(\text{H}_2\text{O})_6]^{2+}$, and the other to the species found at pH 8 (species B).

The EPR parameters of the $\text{Cu}^{2+}/\mathbf{L2}$ and $\text{Cu}^{2+}/\text{cyclen}$ complexes (at $\text{pH} \geq 5$) are similar, pointing to identical coordination environments. The g_i and A_i values are related to the electronic transitions by the factors derived from the ligand field theory [39]: the g_i values increase and the A_i values decrease as the equatorial ligand field becomes weaker or the axial ligand field stronger and this occurs with the simultaneous red-shift of the d–d absorption bands in the electronic spectra [39,40].

Additionally the EPR data obtained in this work for the copper(II) complexes of **L2** and cyclen are quite different from those for $\text{Cu}^{2+}/\text{cyclam}$ also collected in Table 8. In the latter complex the copper has a square planar geometry, with the equatorial plane formed by the four nitrogen atoms of the macrocycle and the metal centre included into the cavity [41]. Indeed, the 12-membered cavity of **L2** and cyclen is too small for the copper centre, and therefore the macrocycle take a folded arrangement with the metal out of the cavity. In the cyclen complex a water molecule or other solution ion completes a five-coordination geometry, while in the $\text{Cu}^{2+}/\mathbf{L2}$ the sulphur of the arm certainly do the same effect. A square-pyramidal geometry is expected for **L2** complexes since in the case of a trigonal-bipyramidal a $g_{\perp} > g_{\parallel}$ and a UV–Vis band in the region 800–850 nm would be observed [42]. Thus, considering the UV–Vis and the EPR data, a square pyramidal geometry

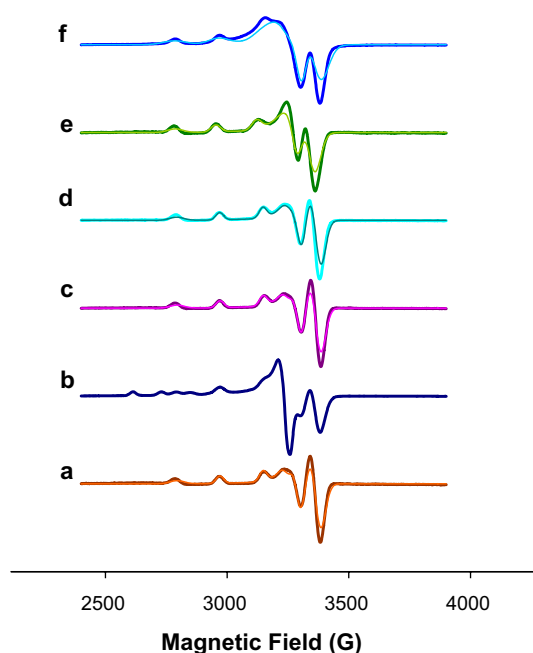


Fig. 7. X-band EPR spectra of copper complexes of **L2** and cyclen in $\approx 1.5 \times 10^{-3} \text{ mol dm}^{-3}$ and 40% DMSO/H₂O solutions (strong lines) and the simulated spectra (smooth lines) at different pH values: (a) $\text{Cu}^{2+}/\text{Cyclen}$, pH 5, at 114.5 K; (b) $\text{Cu}^{2+}/\mathbf{L2}$, pH 5, at 111.6 K; (c) $\text{Cu}^{2+}/\text{Cyclen}$, pH 8, at 105.9 K; (d) $\text{Cu}^{2+}/\mathbf{L2}$, pH 8, at 112.2 K; (e) $\text{Cu}^{2+}/\text{Cyclen}$, pH 12, at 119.4 K and (f) $\text{Cu}^{2+}/\mathbf{L2}$, pH 12, at 107.6 K. All spectra were recorded with microwave power of 2.0 mW, modulation amplitude of 1 mT, and frequency of 9.41 GHz.

is expected for all the complexes studied in this work, and the small changes observed for $\text{Cu}^{2+}/\mathbf{L2}$ versus $\text{Cu}^{2+}/\text{cyclen}$ can be most probably only assigned to distortions in the structure, promoted by a stronger coordination of the thiol group at higher pH.

4. Concluding remarks

A mono-N-substituted cyclen derivative with a 2-ethanethiol pendant arm, 2-[1,4,7,10-tetraazacyclododecan-1-yl]-ethanethiol (**L2**), has been successfully synthesized, being its thiol-protected precursor (**L1**) also characterized in solution and in the solid state. Compound **L2** was characterized by 2D NMR studies and its protonation constants were determined by potentiometry. An analysis of the protonation scheme of **L2** was discussed based on ^{13}C NMR titration. The stability constants of **L2** with Cu^{2+} , Zn^{2+} and Cd^{2+} were determined by potentiometry, and their values follow the usual trend found for cyclen derivatives: $[\text{CuL2}] > [\text{ZnL2}] \approx [\text{CdL2}]$. At physiological pH, the pM values calculated for the metal complexes of **L2** have shown that this ligand is less selective for Cu^{2+} over Zn^{2+} and Cd^{2+} , compared to cyclen and cyclam. Spectroscopic data indicate that **L2** forms penta-coordinated complexes with Cu^{2+} and Zn^{2+} .

In summary, the introduction of a thiol pendant arm in the cyclen backbone has improved the affinity for Cu^{2+} but its selectivity has decreased. Radioactive studies with copper are underway to evaluate the possible use of this ligand for biological applications.

5. Supplementary material

CCDC 636011 contains the supplementary crystallographic data (excluding structure factors) for **L1**. These data can be obtained free of charge via <http://www.ccdc.cam.ac.uk/conts/retrieving.html>, or from the Cambridge Crystallographic Data Centre, 12 Union Road, Cambridge CB2 1EZ, UK; fax: (+44) 1223-336-033; or e-mail: deposit@ccdc.cam.ac.uk.

Acknowledgements

S. Lacerda thanks FCT for the Ph.D. Grant (SFRH/BD/19168/2004). S. Lacerda, M.P. Campello and I. Santos thank Prof. J. Ascenso for NMR discussions. The authors also thank Dr. J. Marçalo for MS measurements and S. Carvalho for the EPR measurements.

References

- [1] (a) C.J. Anderson, in: M.J. Welch, C.S. Redvanly (Eds.), *Handbook of Radiopharmaceuticals: Radiochemistry and Applications*, Wiley, New York, 2003, pp. 401–422 (Chapter 12);
(b) C.J. Anderson, M.J. Welch, *Chem. Rev.* 99 (1999) 2219;
(c) P.J. Blower, J.S. Lewis, J. Zweit, *Nucl. Med. Biol.* 23 (1996) 957.
- [2] (a) L.J. Ackerman, D.X. West, C.J. Mathias, M.A. Green, *Nucl. Med. Biol.* 26 (1999) 551, and references therein;
- (b) J.S. Lewis, A. Srinivasan, M.A. Schmidt, C.J. Anderson, *Nucl. Med. Biol.* 26 (1999) 267;
- (c) B.E. Rogers, H.M. Bigott, D.W. McCarthy, D.D. Manna, J. Kim, T.L. Sharp, M.J. Welch, *Bioconj. Chem.* 14 (2003) 756;
- (d) X. Chen, R. Park, M. Tohme, A.H. Shahinian, J.R. Badind, P.S. Conti, *Bioconj. Chem.* 15 (2004) 41;
- (e) X. Liang, P. Sadler, *Chem. Soc. Rev.* 33 (2004) 246.
- [3] L.A. Bass, M. Wang, M.J. Welch, C.J. Anderson, *Bioconj. Chem.* 11 (2000) 527.
- [4] A. Lewin, J.P. Hill, R. Boetzel, T. Georgiou, R. James, C. Kleanthous, G.R. Moore, *Inorg. Chim. Acta* 331 (2002) 123.
- [5] (a) D. Tschudin, A. Basak, T.A. Kaden, *Helv. Chim. Acta* 71 (1988) 100;
(b) R. Ma, M.J. Welch, J. Reibenspies, A.E. Martell, *Inorg. Chim. Acta* 236 (1995) 75;
(c) R.P. Houser, J.A. Halfen, V.G. Young Jr., N.J. Blackburn, W.B. Tolman, *J. Am. Chem. Soc.* 117 (1995) 10745;
(d) T. Gyr, H.R. Mäcke, M. Herming, *Angew. Chem., Int. Ed. Engl.* 36 (1977) 24.
- [6] (a) L. Maria, A. Paulo, I.C. Santos, I. Santos, P. Kurtz, B. Spingler, R. Alberto, *J. Am. Chem. Soc.* 128 (2006) 14590;
(b) R. Garcia, L. Gano, L. Maria, A. Paulo, I. Santos, H. Spies, J. Biol. Inorg. Chem. 11 (2006) 769;
(c) S. Alves, J.D.G. Correia, I. Santos, B. Veerendra, G.L. Sieckman, T.J. Hoffman, T. Rold, L. Retzloff, J. McCrate, A. Prasanphanich, C.J. Smith, *J. Nucl. Med. Biol.* 33 (2006) 625;
(d) F. Marques, L. Gano, M. Paula Campello, S. Lacerda, I. Santos, L.M.P. Lima, J. Costa, R. Delgado, *J. Inorg. Biochem.* 100 (2006) 270;
(e) S. Alves, J.D.G. Correia, A. Paulo, L. Gano, J. Smith, I. Santos, *Bioconj. Chem.* (2005) 438;
(f) C. Fernandes, S. Seifert, H. Spies, R. Syhre, R. Bergman, L. Gano, I. Santos, *Bioconj. Chem.* 16 (2005) 660;
(g) I. Santos, A. Paulo, J.D.G. Correia, *Top. Curr. Chem.* 252 (2005) 45, *Contrast Agents III: Radiopharmaceuticals—From Diagnostics to Therapeutics*, Springer, Berlin, Heidelberg 2005.
- [7] S. Meegalla, K. Plössl, M.-P. Kung, S. Chumpradit, D.A. Stevenson, D. Frederick, H.F. Kung, *Bioconj. Chem.* 7 (1996) 421.
- [8] G.M. Sheldrick, *SADABS*, Bruker AXS Inc., Madison, WI, USA, 2004.
- [9] Bruker, *SMART and SAINT*, Bruker AXS Inc., Madison, WI, USA, 2004.
- [10] A. Altomare, M.C. Burla, M. Camalli, G. Cascarano, G. Giacovazzo, A. Guagliardi, A.G.G. Moliterni, G. Polidori, R. Spagna, *J. Appl. Cryst.* 32 (1999) 115.
- [11] G.M. Sheldrick, *SHELXL97*, Program for Crystal Structure Refinement, University of Göttingen, Germany, 1997.
- [12] L.J. Ferrugia, *J. Appl. Cryst.* 32 (1999) 837.
- [13] L.J. Ferrugia, *J. Appl. Cryst.* 30 (1997) 565.
- [14] G. Shwardzenbach, W. Flaschka, *Complexometric Titrations*, Methuen & Co, London, 1969.
- [15] G. Shwardzenbach, W. Biedermann, *Helv. Chim. Acta* 31 (1948) 331.
- [16] (a) P. Antunes, P.M. Campello, R. Delgado, M.G.B. Drew, V. Félix, I. Santos, *J. Chem. Soc., Dalton Trans.* (2003) 1852;
(b) K.P. Guerra, R. Delgado, L.M.P. Lima, M.G.B. Drew, V. Félix, *J. Chem. Soc., Dalton Trans.* (2004) 1812;
(c) F. Marques, K.P. Guerra, L. Gano, J. Costa, M.P. Campello, L.M.P. Lima, R. Delgado, I. Santos, *J. Biol. Inorg. Chem.* 9 (2004) 859.
- [17] (a) J. Costa, R. Delgado, M.G.B. Drew, V. Félix, A. Saint-Maurice, *J. Chem. Soc., Dalton Trans.* 12 (2000) 1907;
(b) J. Costa, R. Delgado, M.G.B. Drew, V. Félix, R.T. Henriques, J.C. Waerenborgh, *J. Chem. Soc., Dalton Trans.* 18 (1999) 3253.
- [18] P. Gans, A. Sabatini, A. Vacca, *Talanta* 43 (1996) 1739.
- [19] NIST Standard Reference Database 46, NIST Critically Selected Stability Constants of Metal Complexes Database, Version 5.0, Data collected and selected by R.M. Smith and A.E. Martell, US Department of Commerce, National Institute of Standards and Technology, 1998.

- [20] A.K. Covington, M. Paabo, R.A. Robison, R.G. Bates, *Anal. Chem.* 40 (1968) 700.
- [21] T.J. Lotz, T.A. Kaden, *J. Chem. Soc., Chem. Commun.* (1977) 15.
- [22] T.J. Lotz, T.A. Kaden, *Helv. Chim. Acta* 61 (1978) 1376.
- [23] N.W. Alcock, H.A. Omar, P. Moore, C. Pierpoint, *J. Chem. Soc., Dalton Trans.* (1985) 219.
- [24] Z. Kovacs, D. Sherry, *Synthesis* (1996) 759.
- [25] (a) K. Malesse, A. Loos, *Liebigs Ann.* (1996) 935;
(b) M. Woods, G.E. Kiefer, S. Bott, A. Castillo-Muzquiz, C. Eshelbrenner, L. Michaudet, K. McMillan, S.D.K. Mudigunda, D. Ogrin, G. Tircsó, S. Zang, P. Zhao, D. Sherry, *J. Am. Chem. Soc.* 126 (2004) 9248;
(c) G. Hervé, H. Bernard, N. Le Bris, M. Le Baccon, J.-J. Yaouanc, H. Handel, *Tetrahedron Lett.* 41 (1999) 2571;
(d) J. Rohovec, R. Gyepes, I. Císařová, J. Rudovský, I. Lukeš, *Tetrahedron Lett.* 41 (2000) 1249.
- [26] M. Studer, T.A. Kaden, *Helv. Chim. Acta* 69 (1986) 2081.
- [27] P.J. Davies, K.P. Wainwright, *Inorg. Chim. Acta* 294 (1999) 103.
- [28] (a) W. Clegg, P.B. Iveson, J.C. Lockhart, *J. Chem. Soc., Dalton Trans.* (1992) 3291, and references therein;
(b) E. Kimura, H. Kitamura, T. Koike, M. Shiro, *J. Am. Chem. Soc.* 119 (1997) 10909;
(c) C. Bazzicalupi, A. Bencini, E. Berni, A. Bianchi, S. Ciattini, C. Giorgi, S. Maoggi, P. Paoletti, B. Valtancoli, *J. Org. Chem.* 67 (2002) 9107.
- [29] (a) A.P. Leugger, L. Hertli, T.A. Kaden, *Helv. Chim. Acta* 61 (1978) 2296;
(b) M. Kodama, E. Kimura, *J. Chem. Soc., Dalton Trans.* (1980) 327;
(c) T. Koike, S. Kajitani, I. Nakamura, E. Kimura, *J. Am. Chem. Soc.* 117 (1995) 1210.
- [30] C. Frassinetti, L. Alderighi, P. Gans, A. Sabatini, A. Vacca, S. Ghelli, *Anal. Bioanal. Chem.* 376 (2003) 1041.
- [31] R. Delgado, J.J.R.F. Da Silva, M.T.S. Amorim, M.F. Cabral, S. Chaves, J. Costa, *Anal. Chim. Acta* 245 (1991) 271.
- [32] (a) Ryszard Nazarski, *Magn. Reson. Chem.* 41 (2003) 70, and references cited therein;
(b) R. Clay, S. Corr, M. Micheloni, P. Paoletti, *Inorg. Chem.* 24 (1985) 3330;
(c) A. Bianchi, B. Escuder, E. Garcia-España, S.V. Luis, V. Marcelino, J.F. Miravet, J.A. Ramírez, *J. Chem. Soc., Perkin Trans. 2* (1994) 1253;
(d) C.N. Reilley, *Anal. Chem.* 47 (1975) 2116;
(e) M. Ciampolini, M. Micheloni, N. Nardi, P. Paoletti, P. Dapporto, F. Zanobini, *J. Chem. Soc., Dalton Trans.* (1984) 1357.
- [33] V.J. Thöm, G.D. Hosken, R.D. Hancock, *Inorg. Chem.* 24 (1985) 3378.
- [34] (a) M. Kodama, E. Kimura, *J. Chem. Soc., Dalton Trans.* 116 (1976) 1720;
(b) M. Kodama, E. Kimura, *J. Chem. Soc., Dalton Trans.* (1977) 1473;
(c) M. Micheloni, A. Sabatini, P. Paoletti, *J. Chem. Soc., Perkin Trans. 2* (1978) 828.
- [35] L. Alderighi, P. Gans, A. Ienco, D. Peters, A. Sabatini, A. Vacca, *Coord. Chem. Rev.* 184 (1999) 311.
- [36] K. Miyoshi, H. Tanaka, E. Kimura, S. Tsuboyama, S. Murata, H. Shimizu, K. Ishizu, *Inorg. Chim. Acta* 78 (1983) 23.
- [37] F. Neese, Diploma Thesis, University of Konstanz, Germany, 1993.
- [38] E.I. Solomon, K.W. Penfield, D.E. Wilcox, *Struct. Bonding* 53 (1983) 1.
- [39] (a) A.W. Addison, M. Carpenter, L.K.-M. Lau, M. Wicholas, *Inorg. Chem.* 17 (1978) 1545;
(b) M.J. Maroney, N.J. Rose, *Inorg. Chem.* 23 (1984) 2252.
- [40] P.W. Lau, W.C. Lin, *J. Inorg. Nucl. Chem.* 37 (1975) 2389.
- [41] (a) P.A. Tasker, L. Sklar, *J. Cryst. Mol. Struct.* 5 (1975) 329;
(b) J.C.A. Boeyens, S.M. Dobson, in: Ivan Bernal (Ed.), *Stereochemical and Stereophysical Behaviour of Macrocycles*, vol. 2, Elsevier, Amsterdam, 1987, pp. 1–102.
- [42] M.C. Styka, R.C. Smierciak, E.L. Blinn, R.E. DeSimone, J.V. Passariello, *Inorg. Chem.* 17 (1978) 82.